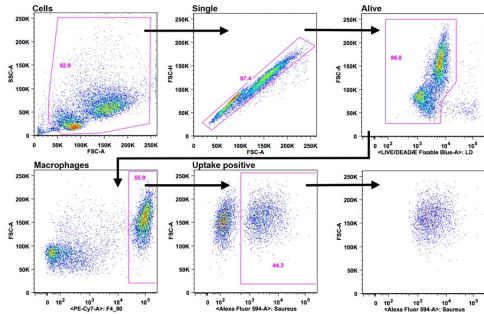
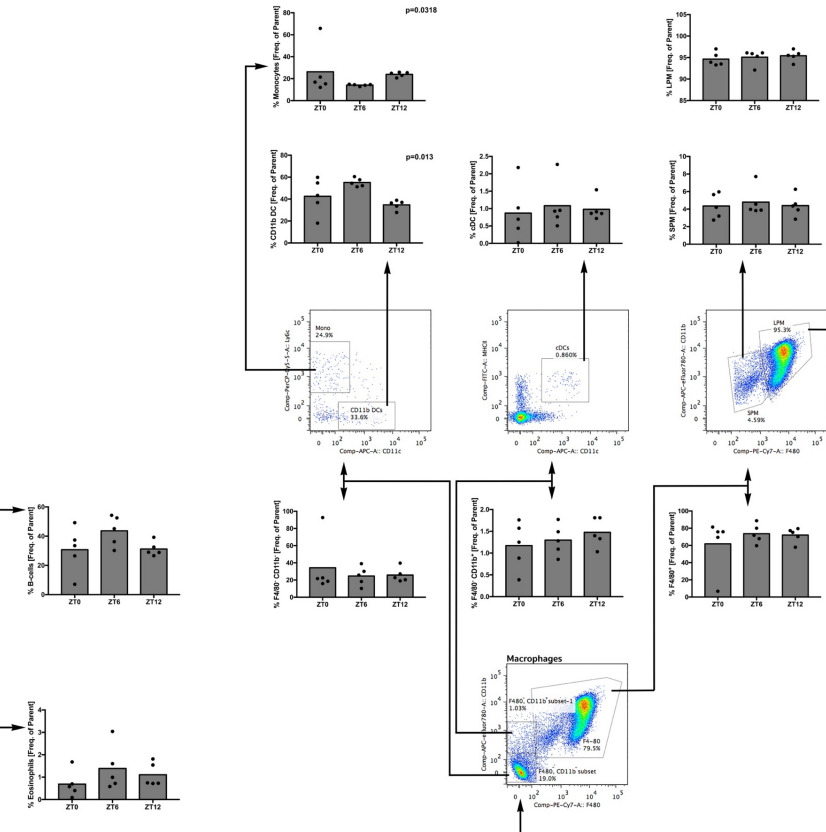
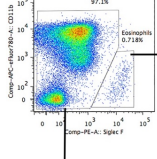
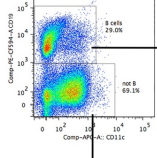
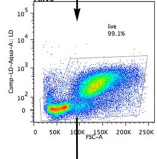
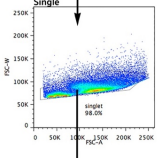
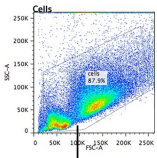


A



B



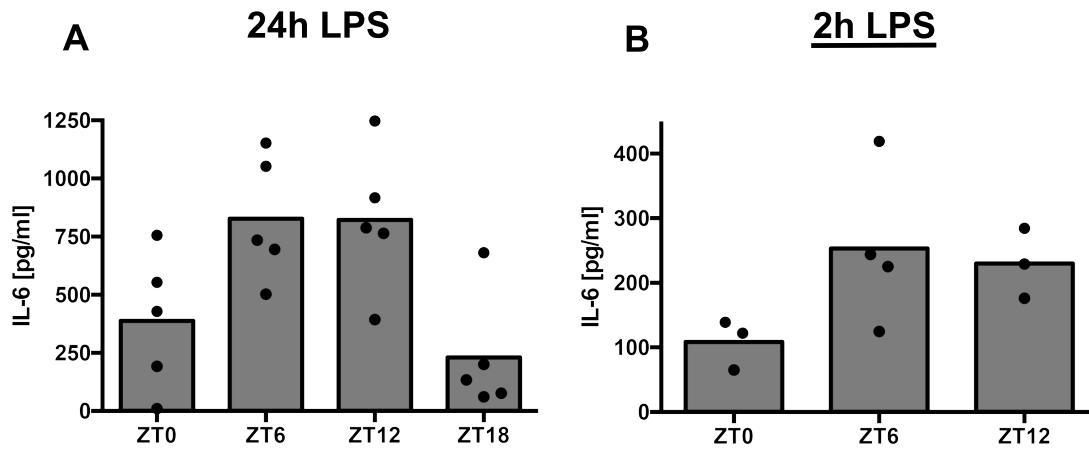
Supplementary Figure S1: Immune cell subsets within the peritoneal cavity display similar abundance over the course of a day.

A) Gating strategy for uptake positive peritoneal macrophages following incubation with fluorescent particles. Debris was gated out via FSC and SSC and cells were further gated on FSC-H and FSC-A to select for single cells. Live/Dead negative, living cells were then separated into F4/80 negative cells or F4/80 positive macrophages, which were further analysed for particle-derived fluorescence. The Mean Fluorescence Intensity (MFI) was analysed in uptake positive cells only. B) Percentage of immune cell subsets found in the peritoneal cavity following extraction at ZT0, ZT6 and ZT12. Gating strategy as indicated in representative FACS analysis plots and quantification of abundance in biological replicates displayed as % of parent population. No statistically significant differences as per Kruskal Wallis one-way ANOVA were found between any of the subsets across time points if not indicated on the graph.

See video file

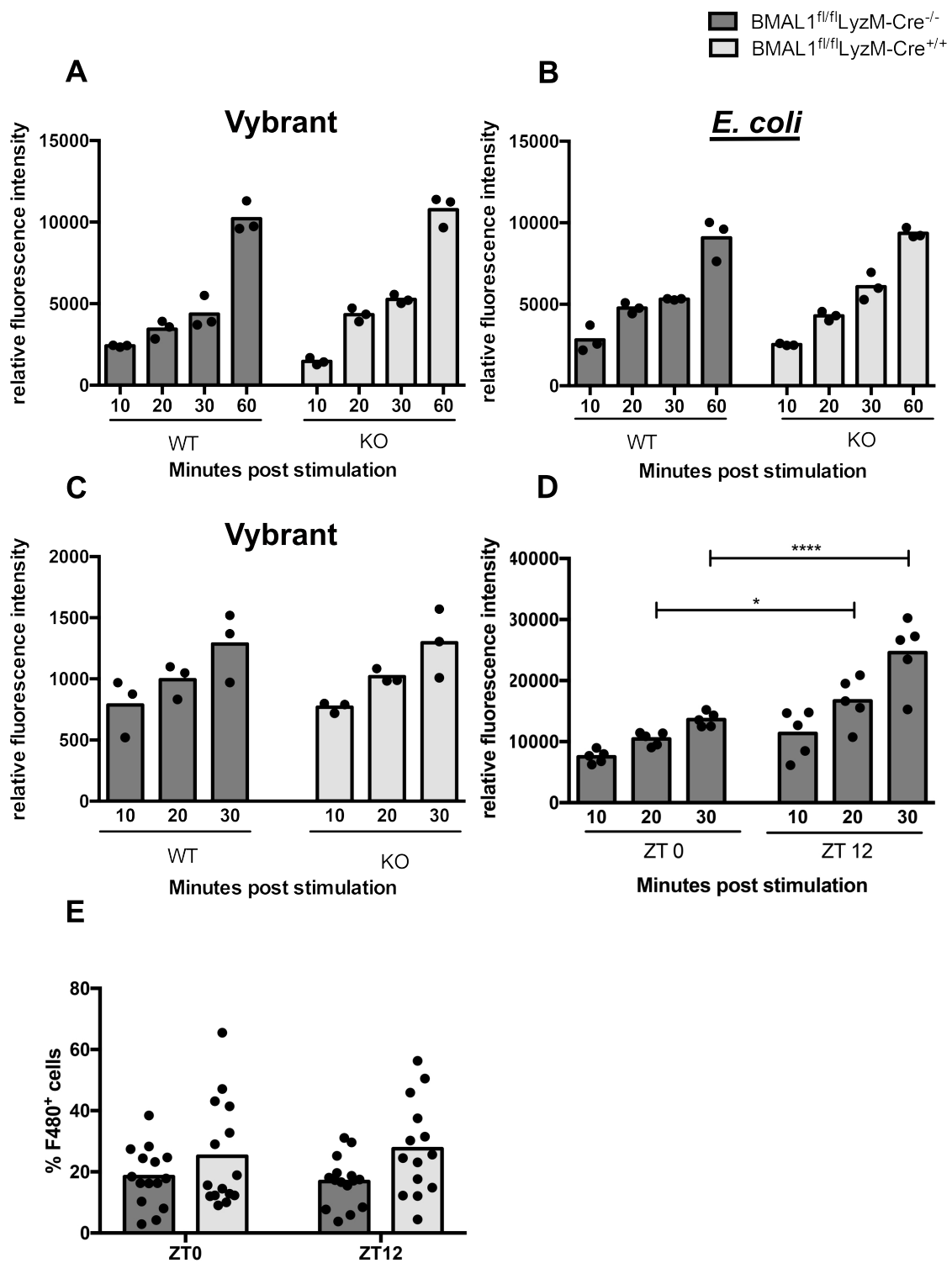
Supplementary Figure S2: Uptake 3-D model.

3-D animation of cumulative uptake data from Z-stack confocal images of mouse peritoneal macrophages stimulated for 1 h with fluorescent *S. aureus* bioparticles (red) and stained with a cell membrane impermeable anti-*S. aureus* antibody (green) as well as membrane (grey) and nuclear (blue) dyes to visualize membrane bound and intracellular particles.



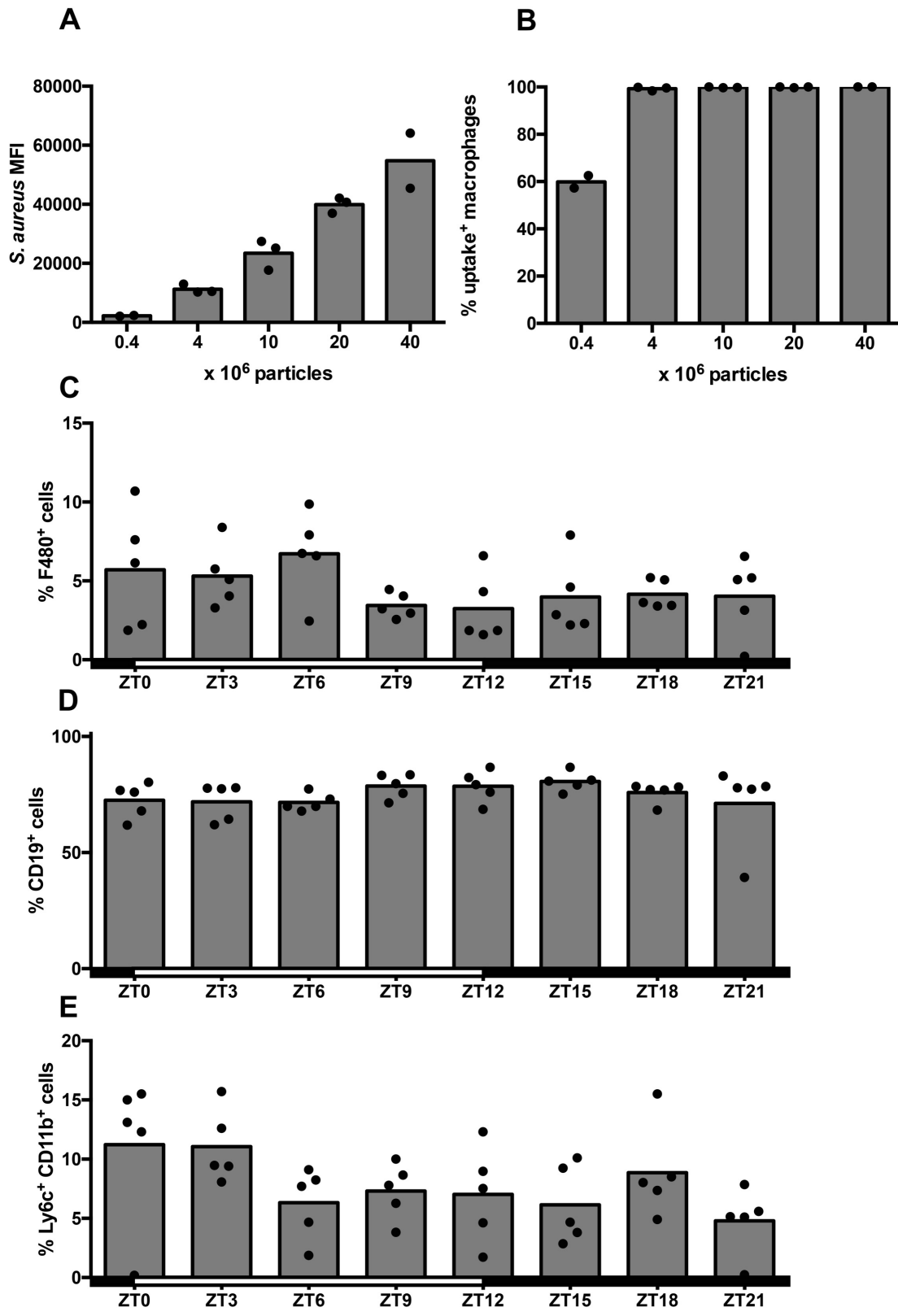
Supplementary Figure S3: *Ex vivo* cytokine production is dependent on time of day.

A, B) Abundance of IL-6 in the supernatant of peritoneal cells extracted at the indicated times and stimulated for 24 h ($p=0.018$) (A) or 2 h ($p=0.101$) (B) with 100ng/ml LPS. Statistical analysis using Kruskal Wallis one-way ANOVA and Dunn's post-hoc multiple comparison.



Supplementary Figure S4: Kinetics of bacterial particle uptake in macrophages and the abundance of F4/80⁺ cells in the peritoneum is not impacted by *Bmal1* deletion.

Fluorescence in cells isolated from BMAL1^{fl/fl}LyzM-Cre^{+/+} or BMAL1^{fl/fl}LyzM-Cre^{-/-} control mice incubated for indicated times with fluorescent material. A) BMDMs incubated with Vybrant ($F_{1,4}=1.046$, $p=0.3643$). B) BMDMs incubated with living *E. coli* (MOI500) ($F_{1,4}=0.1262$, $p=0.7403$). C) Peritoneal macrophages incubated with Vybrant ($F_{1,4}=0.00134$, $p=0.9725$). D) Peritoneal macrophages incubated with Vybrant at ZT0 or ZT12 (ZT effect: $F_{1,24}=32.89$, $p<0.0001$). E) Percentage of F/80 positive cells within the peritoneal lavage at ZT0 and ZT12 ($F_{1,55}=6.487$, $p=0.0137$). Statistical analysis of the genotype effect (if not stated otherwise) using two-way ANOVA and Sidak's multiple comparison test, * $p<0.05$, **** $p<0.0001$.



Supplementary Figure S5: *S. aureus* in vivo titration and immune cell abundance in the peritoneum post stimulation.

A, B) Dose dependency of mean fluorescence intensity in uptake positive ($p < 0.0001$) (A) and percentage of uptake positive ($p = 0.0363$) (B) F4/80⁺ peritoneal cells harvested 1 h post i.p. *in vivo* stimulation with indicated amounts of fluorescent *S. aureus* particles. Statistical analysis using Kruskal Wallis ANOVA. C-D) Immune cell abundance in the peritoneum 1 h post i.p. delivery of 2×10^7 *S. aureus* particles. C) F4/80⁺ Macrophages. D) CD19⁺ B-cells. E) Ly6c⁺CD11b⁺ Monocytes. No statistical significance in the abundance of any of the subsets were found in any of the subsets across time points (Kruskal Wallis one-way ANOVA).